Chapter 2

Marine Aerosol Formation from Biogenic Iodine Emissions*

2.1. Abstract

Elucidation of the mechanisms leading to new particle formation in the marine atmosphere has proved evasive despite intense efforts in recent years. Previous studies implicated dimethyl-sulphide (DMS)-derived H_2SO_4 as the species controlling marine aerosol and cloud condensation nuclei (CCN) production, and consequently, climate change[1]. However, to date, it has proven difficult to conclusively link DMS emissions to new particle formation and consequently, the processes controlling marine particle formation remain undetermined[2-3]. Here, using laboratory experiments, we prove that particle production from condensable iodine-containing vapours (CIVs), deriving from biogenic iodo-carbons emitted by the marine biota, occurs under coastal atmospheric conditions and we illustrate, using modelling studies, that CIVs will influence particle formation over the open ocean, thereby enhancing marine particle production, which in turn, has a potentially significant impact on global radiative forcing.

2.2. Analysis

In terms of the global radiative budget, scattering of incoming radiation by marine aerosols and stratiform clouds contributes most to the radiative balance due to the low albedo of the ocean surface[4]. Further, marine clouds are most susceptible to perturbations resulting from changes in CCN availability which inherently and fundamentally are dependent on the formation of new particles. Hence, the global radiative balance is significantly influenced by the production rate of new particles in the marine boundary layer. There are two steps required for the production of new particles under gas-to-particle conversion processes (secondary particle formation): first, a critical embryo, or thermodynamically stable cluster (TSC) of the order of 1 nm in size, must be formed from the coalescence of precursor vapours (homogeneous nucleation)[5]; and secondly, these stable clusters must grow rapidly enough, either by

coagulation and/or condensation, to quasi-stable particle sizes of 3-4 nm (particle formation) before they are diffusion-scavenged by the pre-existing aerosol[6] (the diffusivity of the clusters decreases as $1/d^2$). Once new particles reach sizes of a few nanometers, there is a net increase in the particle number concentration.

Recent simulations of ternary H_2SO_4-H_2O-NH_3 nucleation[7] have shown that under typical atmospheric concentrations of H_2SO_4, nucleation of TSCs can readily occur; however, production of new particles by condensation-growth is unlikely due to insufficient supply of H_2SO_4. While H_2SO_4 could be responsible for the production of TSCs, other vapours are required for particle production. The most comprehensive studies[8] into marine aerosol nucleation have focused on coastal environments, where regular and intense particle production events are encountered due to the higher intensity of biological processes in coastal areas. These studies found particle production to be independent of peak H_2SO_4 concentrations[9], suggesting a hitherto unaccounted marine particle production mechanism. Experimental measurements on new particle composition have ruled out a chemical composition dominated by H_2SO_4[10], and identified iodine in these particles[11]. Consequently, the production of particles in the coastal zone by condensable iodine vapours (CIVs) resulting from the photolysis of biogenic CH_2I_2 has been proposed[8].

To test this hypothesis, we conducted laboratory experiments in the Caltech smog chamber[12] into the particle production ability of CH_2I_2 undergoing photolysis in the presence of ozone and we present new laboratory results confirming this mechanism as a viable mechanism for particle production down to atmospheric concentrations[8]. No particles were formed unless CH_2I_2, O_3, and UV radiation were simultaneously present in the chamber. When UV radiation was introduced after CH_2I_2 and O_3 had been mixed throughout the chamber, rapid homogenous nucleation occurred, followed

by condensation and coagulation growth. This behavior was observed for all experiments for CH_2I_2 levels, from 50 ppb down to the lowest CH_2I_2 concentration achievable in this chamber of 0.015 ppb (~4 x 10^8 molecules cm^{-3}). Decreasing the CH_2I_2 concentration did not change the nucleation or growth phenomenology but resulted in longer time scales for both processes.

Particles formed under dry conditions possessed a fractal morphology, while particles formed under humid conditions (RH ~ 65%) were more compact and dense. No other significant differences in the nucleation or growth behaviour as a function of humidity was observed. Reducing the intensity of the UV radiation slowed the particle formation processes without changing their qualitative features. Analysis of the resultant aerosol chemical composition, using an aerosol mass spectrometer (AMS), revealed the following detected *m/z* peaks: OH^+, H_2O^+, I^+, HI^+, IO^+, HIO^+, IO_2^+, HIO_2^+, HIO_3^+, IO_5^+, I_2^+, I_2O^+, and $I_2O_3^+$ (Figure 2.1). These peaks are consistent with particles composed of iodine oxides and/or iodine oxyacids, and possibly also water. Particle composition did not change with particle size or time in the experiment.

The chemical mechanism associated with the particle production is presented in Figure 2.2. There are three possible pathways to form CIVs: (1) CH_2I_2 is rapidly photolysed, releasing an I atom which reacts with O_3 to produce IO. IO, in turn, reacts with itself to produce OIO which can nucleate to produce I_2O_4 and higher order iodine oxide polymers; (2) IO can also self-react to produce I_2O_2 which can participate in aerosol formation; and (3) IO can react with HO_2 to produce condensable HOI. At the lowest concentrations of less than 20-200 ppt CH_2I_2, HOI is the dominant CIV, while iodine oxides dominate at higher concentrations. These new laboratory results prove for the first time that nucleation and condensation of CIVs occurs under atmospheric

coastal conditions, and that this mechanism must be considered viable in terms of contributing to the marine aerosol population.

Estimates[14-17] of the global flux of iodine from macroalgae are of the order of 10^7-10^8 g yr^{-1}, but this source is limited to coastal zones. Microalgae (phytoplankton), on the other hand, are spread all over the ocean and are estimated to contribute 10^9-10^{10} g yr^{-1}. The global ocean source, however, is estimated[14-17] to be 10^{11}-10^{12} g yr^{-1}, but the major contributor to this source of iodine-- in addition to micro and macro algae-- is currently unidentified, although there is strong evidence that bacteria can synthesize CH_3I, which could account for the missing source[17]. Nevertheless, taking a global marine source of 10^{12} g yr^{-1} and a globally-averaged marine surface-mixed-layer height of 300 m, the source rate of iodine atoms is estimated at 1.4 x 10^3 atoms cm^{-3} s^{-1}. This open ocean source of iodine atoms compares favourably to the recent estimate of 1 x 10^4 atoms cm^{-3} required to explain the observed concentration of IO and OIO (up to 1.6 x 10^8 cm^{-3}) over the open ocean[18,19].

We simulate, using a marine aerosol model, the production of new particles resulting from condensation of CIVs onto TSC embyros. The simulation (Figure 2.3) is started just before sunrise and as DMS is photochemically destroyed, H_2SO_4 production also increases, leading to a peak concentration of 2.5 x 10^6 molecules cm^{-3} . At these typical H_2SO_4 concentrations, the concentration of TSCs reaches a maximum of ≈ 5000 cm^{-3}, resulting from a peak nucleation rate of 4 cm^{-3} s^{-1}; however, barely-detectable new particle formation results in sizes larger than 3 nm. When an additional CIV source (Q) of 10^3 cm^{-3} s^{-1} is included, slight particle production results after a few hours resulting from an enhancement in condensable vapours of 0.5 x 10^6 cm^{-3}. Increasing Q to 5, 10 and 25 x 10^3 molecules cm^{-3} s^{-1} leads to a CIV concentration of 2.5, 5 and 12 x 10^6 molecules cm^{-3}, and increases the

particle concentration from 518 cm^{-3} to 555 cm^{-3}, 614 cm^{-3} and 804 cm^{-3}, respectively. Clearly, increasing the source rate of CIVs significantly increases the production rate of new particles.

The initial and final aerosol size distributions are given in Figure 2.4 for all simulations. As the CIV vapour concentration increases, the final concentration of the nucleation mode increases, as does the mean modal-size (up to 6 nm). At a condensable vapour concentration of 2.4 x 10^6 cm^{-3} (Q=0), the nucleation mode comprising TSCs, initially 1 nm in size, cannot grow into sizes larger than 3 nm (mode diameter) since the growth rate is slow (0.2 nm $hour^{-1}$) relative to the coagulation sink[20] (2 x 10^{-3} s^{-1} for a 1 nm particle, decreasing to 2 x 10^{-4} s^{-1} for a 3 nm particle). At a vapour concentration of 14 x 10^6 cm^{-3} (Q=25 x 10^3 molecules cm^{-3} s^{-1}), the growth rate is significantly faster (1.1 nm $hour^{-1}$). Therefore, it takes $1/5^{th}$ of the time to reach sizes of 3 nm where particles can survive 10 times longer. Similarly, as the particle grows to 6 nm, its loss rate is reduced even further to 4 x 10^{-5} s^{-1}. In essence, this additional vapour source carries the nuclei over a coagulation loss barrier, resulting in a higher probability of the new particles surviving. If dimer-nucleation of CIVs is considered[21], nucleation rates are predicted to increase to 10^2 cm^{-3} s^{-1} for a CIV concentration of 10^6 cm^{-3}, increasing further to 10^4 cm^{-3} s^{-1} for a CIV concentration of 10^7 cm^{-3}; therefore, CIVs are likely to also contribute to the nucleation process.

Overcoming the coagulation loss barrier essentially increases the number and lifetime of condensation sites for CCN production during the next days' cycle. Typically, the CCN concentration for clean marine air is 50 cm^{-3} to 100 cm^{-3}, accounting for 10-20% of the aerosol population. The increase in the net input of particles into the aerosol population is likely to result in a similar percentage increase

in available CCN (corresponding to ≈10% of the new particles surviving to CCN sizes). Therefore, changes in the source rate of biogenic CIVs associated with global change are likely to significantly influence the CCN population. In fact, studies into the emissions of iodo-carbons from marine biota have shown that emissions can increase by up to five times resulting from changes in environmental conditions associated with global change[14]. Therefore, increasing the source rate of CIVs five-fold will result in an increase in marine aerosol and CCN concentrations by the order of 20-60 %.

Changes in cloud albedo resulting from changes in CCN concentrations of this magnitude can lead to an increase in global radiative forcing, similar in magnitude, but opposite in sign to the forcing induced by greenhouse gases[22].

Although in some regions there is evidence for marine particle production from organic species[23], the proposed contribution of CIVs to the marine aerosol is most strongly supported by field measurements of marine aerosol composition[24-28]: iodine enrichment factors as high as 1000 relative to bulk sea-water have been found in marine aerosols globally, reaching factors as high as 33,000 in coastal zones. This work confirms a new aerosol nucleation mechanism involving CIVs in coastal regions and suggests that CIVs enhance the production of particles in conjunction with DMS-derived H_2SO_2 nucleation over remote oceans. CIVs could also contribute to the remote-ocean nucleation; however, to confirm this, more theoretical and experimental advances into understanding the atmospheric iodine cycle must first be achieved.

2.3. Methods

2.3.1. Laboratory Experiments

Aerosol formation from the photolysis of CH_2I_2 in the presence of O_3 was investigated in the Caltech indoor chamber. This facility has been described

previously[12] and consists of dual, 28 m^3 chambers illuminated by 300 1.22 m fluorescent blacklights which are used to simulate the UV and near UV regions of ambient sunlight. The UV light intensity in the chamber was measured with a portable spectroradiometer (LI-1800, LI-COR, Lincoln, Nebraska), and was about 1.2 times the maximum intensity reaching the Earth's surface with a Zenith angle of 0°, except for one low radiation experiment which was performed with ¼ of the full intensity. The reaction chamber was filled with particle-free dry air at 20°C that had been scrubbed of both volatile organic compounds (VOCs) and NO_x. CH_2I_2 (99% purity) was obtained from Sigma-Aldrich (St. Louis, Missouri), dissolved in hexafluorobenzene (Sigma-Aldrich, 99% purity), and the solution was evaporated into clean dry carrier air and injected into the chamber. After O_3 injection and allowing sufficient time for reactant mixing, the experiment was initiated by switching on the UV lights.

The evolution of the particle number concentration, number distribution, and hygroscopicity was monitored via condensation particle counters, differential mobility analyzers, and a tandem differential mobility analyzer, respectively, as described[12]. CH_2I_2 concentrations of 0.015 ppb resulted in particle growth up to 30 nm (mode diameter) while for concentrations of 50 ppb, the maximum mode size reached was 200 nm. Particle composition was monitored using an Aerodyne Aerosol Mass Spectrometer (AMS)[29]. Briefly, the AMS uses an aerodynamic lens inlet to focus the sampled particles into a narrow beam which is then introduced into a high vacuum chamber while the air is differentially pumped. The particles are vaporized upon impaction on a heated, roughened molybdenum cartridge heater under high vacuum (10^{-7} Torr) at about 600°C. The vaporized species are then electron impact ionized (70 eV electrons), and the positive ions produced are mass analyzed with a quadrupole

mass spectrometer. Particle aerodynamic diameter is determined via particle time-of-flight. The AMS can produce two types of data: mass spectra of the species present in/on the aerosol, and mass-weighed size distributions vs. aerodynamic diameter at a series of *m/z* peaks of the mass spectrometer. The AMS used in these experiments was able to detect particles between about 40 nm and 1 micron, with a minimum detectable concentration of about 0.5 μg m^{-3}. The AMS was calibrated for particle size with polystyrene latex spheres (Duke Scientific, Palo Alto, California).

2.3.2. Aerosol Modeling

The model used in this study is a AEROFOR[7], a Lagrangian-based 27-bin sectional box model which includes gas-phase chemistry and aerosol dynamics. The following processes are considered: (1) DMS surface flux; (2) gas-phase oxidation of DMS to SO_2/SO_3; (3) gas-phase oxidation of SO_2/SO_3 to H_2SO_4; (4) homogeneous nucleation of H_2SO_4, H_2O and NH_3; (5) condensation of CIVs, MSA, H_2SO_4 and H_2O onto pre-existing particles; (6) direct reaction of SO_2 with particles; (7) Brownian coagulation of particles; and (8) dry deposition to the sea surface. Full details can be found in Ref. 7 and references therein. There are no cloud or precipitation processes included, nor heterogeneous removal of SO_2. The simulations are initialized with a typical marine aerosol concentration of 510 cm^{-3} comprising an Aitken mode, accumulation mode, sea-salt jet drop mode and sea-salt film-drop mode, DMS concentrations of 20 ppt, and NH_3 and SO_2 concentrations of 16 and 5 ppt, respectively. The air parcel undergoes adiabatic cycling in the boundary layer with relative humidity ranging from 70% at the surface to 99% at the top of the boundary layer.

2.4. Acknowledgements

This work was funded by the European Commission, the Finnish Academy, the

U.S. Department of Energy and the Environmental Protections Agency, Ireland.

2.5. References

1. Charlson, R.J., Lovelock, J.E., Andreae, M.O. & S.G. Warren, Oceanic phytoplankton, atmospheric sulphur, cloud albedo and climate, *Nature*, **326,** 655-661, 1987.

2. Katoshevski, D., Nenes, A. & Seinfeld, J.H., A study of processes that govern the maintenance of aerosols in the marine boundary layer, J. *Aerosol. Sci.*, **30**, 503-532, 1999.

3. Capaldo, K.P., Kasibhatla, P. & Pandis, S. N., Is aerosol production within the remote marine boundary layer sufficient to maintain observed concentrations? *J. Geophys, Res.,* **104,** 3483-3500, 1999.

4. Slingo, A., Sensitivity of the Earth's radiation budget to changes in low clouds, *Nature*, **343***,* 49-51, 1990.

5. Korhonen, P., Kulmala, M., Laaksonen, A., Viisanen, Y., McGraw, R. & Seinfeld, J.H.*,* Ternary nucleation of H_2SO_4, NH_3, and H_2O in the atmosphere, *J. Geophys. Res.,* **104 (D21)**, 26349-26353, 1999.

6. Kulmala, M., Pirjola, L. & Mäkelä, J.M., Stable sulphate clusters as a source of new atmospheric particles. *Nature*, **404**, 66-69, 2000.

7. Pirjola, L., O'Dowd, C. D., Brooks, I. M. & Kulmala, M., Can new particle formation occur in the clean marine boundary layer?, *J. Geophys. Res.,* **105**, 26531-26546, 2000

8. O'Dowd, C.D., Hameri, K., Makela, J.M., Pirjola, L., Kulmala, M., Jennings, S.G., Berresheim, H., Hansson, H.C., de Leeuw,G., Kunz, G.J., Allen, A.G., Hewitt, C.N., Jackson, A., Viisanen, Y. & Hoffmann, T. A dedicated study of new particle

formation and fate in the coastal environment (PARFORCE): Overview of objectives and achievements, *J. Geophys. Res*., **107 (D19)**, 2002.

9. Berresheim, H., Elste, T., Tremmel, H.G., Allen, A.G., Hansson, H.C., Rosman, K., Dal Maso, M., Makela, J.M., Kulmala, M., O'Dowd, C.D., Gas-aerosol relationships of H_2SO_4, MSA and H: Observations in the coastal marine boundary layer at Mace Head, Ireland, *J. Geophys. Res*., **107 (D19),** 2002.

10. Väkevä, M., Hämeri, K. & Aalto, P., Hygroscopic properties of nucleation mode and Aitken mode particles during and outside nucleation bursts in west coast of Ireland. *J. Geophys. Res.,* **107 (D19),** 2002.

11. Mäkelä, J.M., Hoffmann, T., Holzke, C., Vakeva, M., Suni, T., Mattila, T., Aalto, P.P., Tapper, U., Kauppinen, E.I. & O'Dowd, C.D., Biogenic iodine emissions and identification of end-products in coastal ultrafine particles during nucleation bursts, *J. Geophys. Res*., **107 (D19),** 2002

12. Cocker, D.R., Flagan, R.C. & Seinfeld, J.H., State-of-the-art chamber facility for studying atmospheric aerosol chemistry, *Env. Sci. Technol.* **35,** 2,594-2,601, 2001.

13. Carpenter, L.J. *et al.*, Short-lived alkyl iodides and bromides at Mace Head, Ireland: Links to biogenic sources. *J. Geophys. Res.,* **104**, 1679-1689, 1999.

14. Laturnus, F., Giese, B., Wiencke, C. & Adams, F., Low molecular-weight organoiodine and organobromine compouds released by polar macroalgae – the influence of abiotic factors. *Fres. J. Anal., Chem.,* **368**, 297-302, 2000.

15. Giese, B., Laturnus, F., Adams, F.C. & Wiencke, C., Release of volatile iodinated C_1-C_4 hydrocarbons by marine macro from various climate zones. *Environ. Sci. Technol.,* **33**, 2432-2439, 1999,

16. Goodwin, K.D., North, W.J. & Lidstrom, M.E., Production of bromoform and dibromomethane by Giant Kelp: Factors affecting release and comparison to anthropogenic bromine sources, *Limnol Oceanogr,* **42**, 1725-1734, 1997.

17. Anache, S., Kamagata, Y., Kanagawa, T. & Kimuramatsu, Y., Bacteria Mediate Methylation of Iodine in Marine and Terrestrial Environments *App. Environ. Microbio.,* **67**, 2718-2722, 2001.

18. McFiggans, G., Plane, J.M.C., Allan, B.J., Carpenter, L.J., Coe, H. & O'Dowd, C.D. A model study of Iodine chemistry in the marine boundary layer, *J. Geophys. Res*., **105**, 14371-14386, 2000.

19. Allan, B.J., Plane, J.M.C. & McFiggans, G., Observations of OIO in the remote marine boundary layer*, Geophys. Res. Letts.,* **27**, 2001.

20. Dal Maso, M., Kulmala, M., Lehtinen, K.E.J., Makela, J.M., Aalto, P. & O'Dowd, C.D. Condensation and coagulation sinks and the formation of nucleation mode particles in coastal and boreal forest boundary layers. *J. Geophys. Res*., **107 (D15)**, 2001.

21. Lushnikov, A.A., & Kulmala, M., Nucleation controlled formation and growth of disperse particles, *Phys. Rev. Letters,* **81**, 5165-5168, 1998.

22. Houghton, J.T., *et al*., Climate Change 2001 – The Scientific Basis, Cambridge University Press, Cambridge, 2001.

23. Leck, C., & Bigg, E. K. Aerosol production over remote marine areas - A new route. *Geophys. Res. Lett*. **23**, 3577-358, 1999.

24. Murphy, D.M., Thomson, D.S. & Middlebrook, A.M., Bromine, iodine and chlorine in single aerosol particles at Cape Grim. *Geophys. Res. Lett.,* **24**, 3197-3200, 1997.

25. Gäbler, H.E., & Heumann, K.-G., Determination of particulate iodine in aerosols from different regions by size fractioning impactor sampling and IDMS. *Int. J Anal. Chem.* **50**, 129-146, 1993.

26. Wimschneider, A. & Heumann, G, Iodine: speciation in size fractioned atmospheric particles by isotope dilution mass spectrometry. *Fres. J. Anal., Chem.,* **353**, 191-196 1995.

27. Baker, A.R., Thompson, D., Campos, M.L.A.M., Parry, S.J. & Jickells, T.D., Iodine concentration and availability in atmospheric aerosol *Atmos. Environ.*, **34**, 4331-4336, 2000.

28. S. Huang, Arimoto, R. & Rahn, K.A., Sources and source variations for aerosol at Mace Head, Ireland *Atmos. Environ.*, **35**, 1421-1437, 2001.

29. Jayne, J. T, Leard, D.C., Zhang, X.F., Davidovits, P., Smith ,K.A., Kolb, C.E. & Worsnop, D.R. Development of an aerosol mass spectrometer for size and composition analysis of submicron particles, *Aerosol Science and Technology*, **33**, 49-70, 2000.

30. Bloss, W.J., Rowley, D.M., Cox, R.A. & Jones, R.L., Kinetics and Products of the IO Self-Reaction*, J. Phys. Chem. A,* **105**, 7,840-7,854, 2001.

Figure 2.1. Observed aerosol mass spectrum from chamber experiments as measured by the AMS. The aerosol measured resulted from the photo-oxidation of CH_2I_2 in the presence of O_3 in pure laboratory air. The observed peaks are consistent with particles composed of iodine oxides and/or iodine oxyacids, and possibly also water. The molybdenum oxide peaks observed in the spectrum are probably due to the oxidation of the molybdenum particle vaporizer of the AMS by iodine oxyacids contained in the sampled particles.

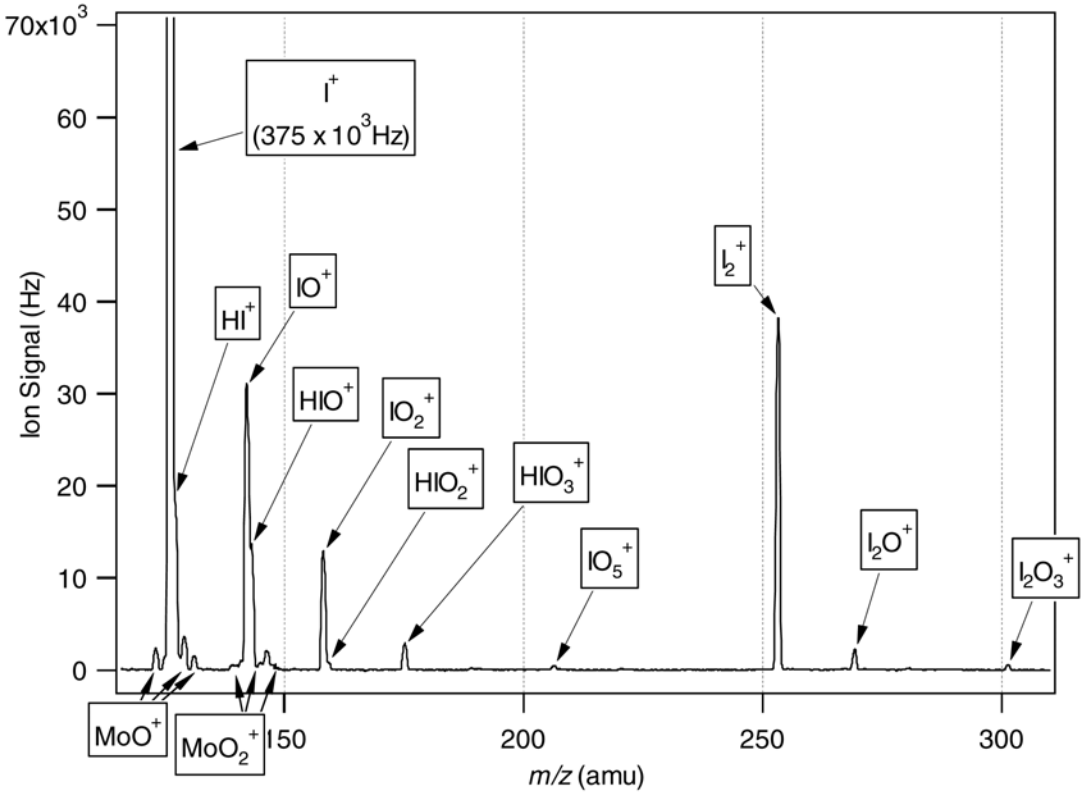

Figure 2.2. Chemical pathway from CH_2I_2 to aerosol production based on the current state of knowledge of the gas phase chemistry. Current quantitative rates are given in Refs. 18 and 30.

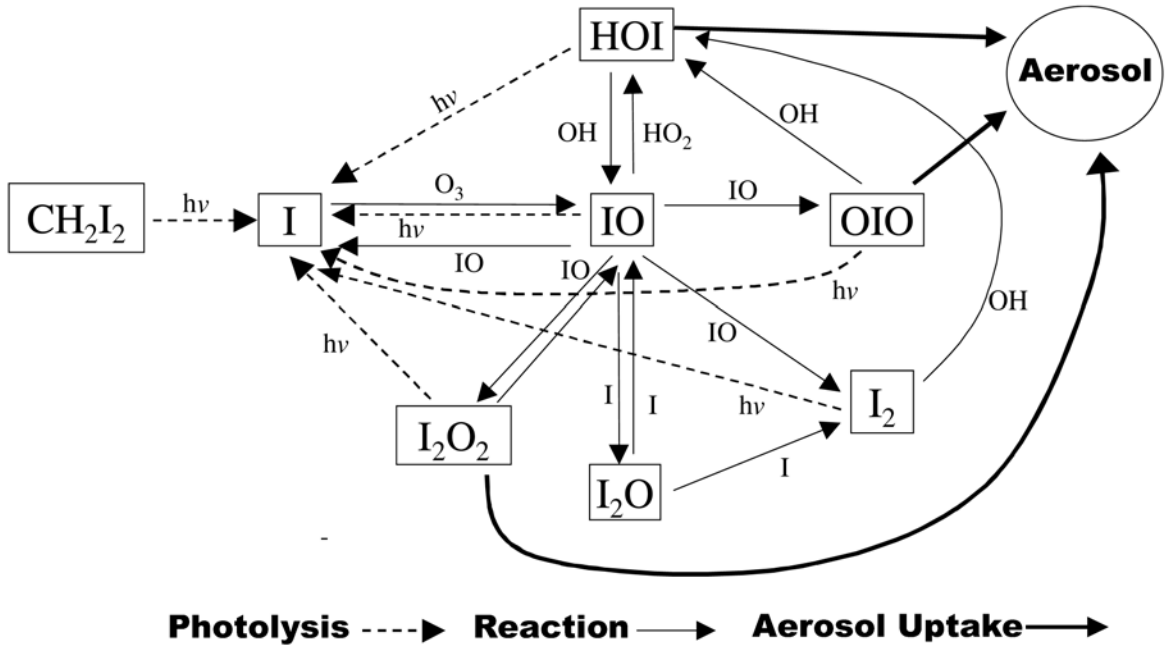

Figure 2.3. Model simulations of condensable vapor and aerosol concentrations in the marine boundary layer. (a) Combined H_2SO_4 and CIV concentration for CIV source rates of 0, 10^3, 5 x 10^3, 10^4 and 2.5 x 10^4 molecules cm^{-3} s^{-1} and a DMS concentration of 20 ppt (5.6 x 10^8 molecules cm^{-3}). Oscillations in the vapor concentration occur due to the variation in the pre-existing aerosol condensation sink as the aerosol surface area responds to changes in relative humidity during air parcel cycling through the boundary layer. (b) Predicted particle concentration (cm^{-3}) at sizes larger than 1 nm (N_{total}), including thermodynamically stable clusters; and detectable particle sizes of 3 nm and greater (N_3) for CIV source rates of 0, 10^3, 5 x 10^3 , 10^4 and 2.5 x 10^4 molecules cm^{-3} s^{-1}.

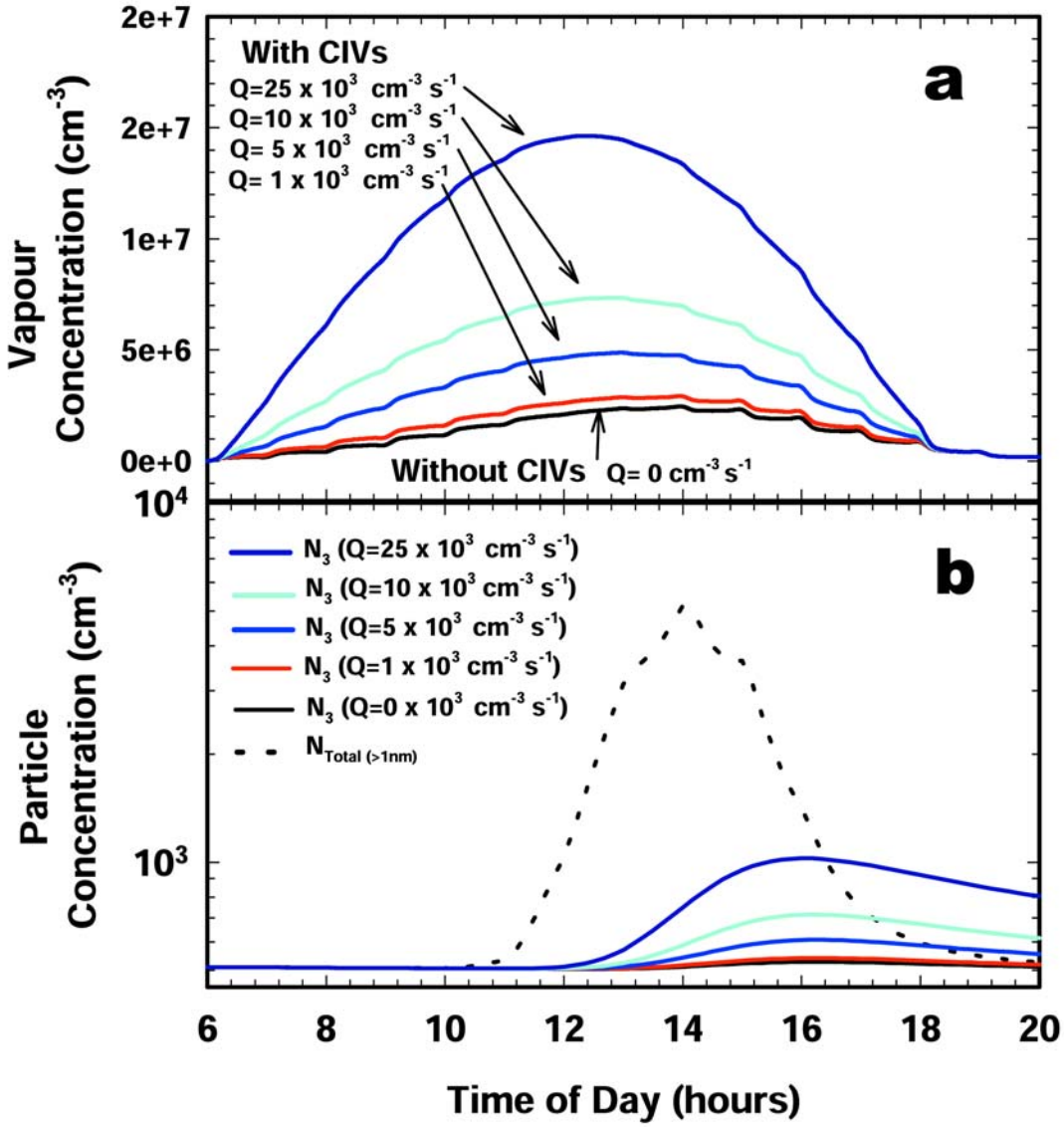
With CIVs
Q=25 x 10^3 cm^-3 s^-1
Q=10 x 10^3 cm^-3 s^-1
Q= 5 x 10^3 cm^-3 s^-1
Q= 1 x 10^3 cm^-3 s^-1
Without CIVs Q= 0 cm^-3 s^-1
a
Vapour Concentration (cm^-3)
2e+7
2e+7
1e+7
5e+6
0e+0
10^4
N3 (Q=25 x 10^3 cm^-3 s^-1)
N3 (Q=10 x 10^3 cm^-3 s^-1)
N3 (Q=5 x 10^3 cm^-3 s^-1)
N3 (Q=1 x 10^3 cm^-3 s^-1)
N3 (Q=0 x 10^3 cm^-3 s^-1)
NTotal (>1nm)
b
Particle Concentration (cm^-3)
10^3
6
8
10
12
14
16
18
20
Time of Day (hours)

Figure 2.4. Predicted aerosol size distributions before (06:00 hours), during (14:00 hours) and after (20:00 hours) the particle production period with CIV source rates (Q) of 0, 10^3, 5 x 10^3 , 10^4 and 2.5 x10^4 molecules cm^{-3} s^{-1}. Also shown is the maximum TSC concentration during peak sulphuric acid production period (note different scale). The coagulation sink (the rate of loss of particles per second due to coagulation with the pre-existing aerosol) as a function of particle size is superimposed on the figure.